

Effect of contact stress on fretting fatigue behavior of 35CrMoA steel under multiaxial non-proportional paths

Zhiqiang Zhou¹, Xiaoshan Liu², Guoqiu He², Bin Ge¹, Peiwen Le², Jingquan Li¹, Jiaqi Pan¹, and Yang Yang¹

¹Affiliation not available

²Tongji University

May 26, 2020

Abstract

This study investigated the fretting fatigue behavior and mechanism of 35CrMoA steel of different contact stresses under diamond and square loading paths in the form of curved surface contact. The results show that multiple crack sources will initiate on the subsurface of the specimen under the combined effect of contact stress and cyclic stress. Under low contact stress, only one crack source dominates, causing the instantaneous fracture zone to be biased to the other side of the main crack source. Under high contact stress, the crack sources in both fretting zones play a dominant role, making the shape of the instantaneous fracture zone into a nearly circular shape with better symmetry; At the beginning of the fretting fatigue, cracks only propagate in the cross-section where they form. When they propagate to a certain depth, a component that propagates in the longitudinal direction will be generated.

Nomenclature: CSZ, crack source zone; CPZ, crack propagation zone; IFZ, instantaneous fracture zone; DP, diamond pat

INTRODUCTION

Fretting refers to a very small relative displacement (in the order of microns, usually 5-50 microns) between two surfaces in contact with each other under a certain contact stress.¹⁻³ Fretting fatigue is an accelerated failure process under the combined action of fretting wear and cyclic stress.^{4,5} In many practical engineering applications, such as the aerospace industry,⁶ the machinery industry,⁷ the transportation industry⁸ etc, there are inevitable vibrations and small relative movement between different contact parts of components,⁴ the interaction causes cracks to easily occur at the contact points, which causes fatigue fracture of the material. The fretting fatigue process is essentially a combination of fretting wear and fatigue caused by the presence of contact stress and cyclic stress. Fretting plays a nonnegligible role in the initiation and propagation of cracks, leading to material failure in advance,⁹ therefore, fretting has a great impact on fatigue life. The current researches on fretting fatigue are mainly focused on the effect of different influencing factors on different materials, and it is generally believed that the factors that have a greater effect on fretting fatigue are contact stress, displacement amplitude, cyclic stress, coefficient of friction, material microstructure, temperature and humidity,¹⁰⁻¹² such as C. Giummarra⁶ and Sachin R. Shinde,¹³ et al. studied the effects of different microstructures of different aluminum alloys on fretting fatigue life, Yang¹⁴ and Jin¹⁵ et al. reported that the effect of contact stress on the fretting fatigue process of different materials. In addition, many studies had also used the finite element method to simulate the stress and strain changes of the fretting process, analyzed the fretting fatigue mechanism on the basis of experiments, and had proposed some fretting fatigue life prediction models based on plain fatigue life models, wear damage, and crack initiation and propagation processes.^{14,16,17} In the process of analyzing fretting fatigue, the fretting maps

had a great effect on analyzing the fretting mechanism and fretting fatigue behavior prediction of materials. Z.R. Zhou¹⁸ et al. made a good summary of the types and development process of fretting map, and Sachin Shinde¹⁹ et al. also made a supplement to the development of fretting map.

35CrMoA steel is a medium carbon alloy structural steel that has both good hardenability and good toughness. It's also featured in high static strength, high fatigue limit and excellent stress-rupture properties at high temperature. Therefore, it was widely used for important structural parts such as large cross-section gears, heavy-duty transmission shafts, and turbine generator main shafts.²⁰ In recent years, due to the requirements of high-speed railways, 35CrMoA steel had been used to manufacture the axles of high-power electric locomotives. In actual operation, due to the close cooperation between this component and its tight fittings, composite fretting usually occurred at the contact parts. Therefore, the performance research of 35CrMoA steel must be carried out in accordance with the actual conditions. Currently, some studies had been done on the fretting fatigue of steels. For example, GH Farrahi²¹ et al. studied the fretting fatigue behavior of 316L stainless steel under the combination of bending and tensile load, and analyzed the effect of grain size in fretting fatigue process; Teng²² et al. investigated the high-cycle fretting fatigue behavior of GCr15 and performed 2D and 3D analysis of the fretting area morphology; Kozo Nakazawa²³ et al. reported the effect of contact stress on austenitic stainless steel, and concluded that the effect of relatively low contact stress on the fretting fatigue life can be neglected, and at high contact stress, plain fatigue experiments performed before fretting fatigue test can increase fretting fatigue life. For 35CrMoA steel, there were limited studies referring its fretting fatigue performance. Liu²⁴ et al. used experimental and finite element analysis methods to study the multiaxial fretting fatigue of 35CrMoA steel, and obtained that with the increase of contact stress, the fretting fatigue life tended to decrease first, then rose and decreased again at the next stage, and stress concentration occurs at the edge of the contact area; Tian²⁵ and Lv²⁶ et al. also investigated the multiaxial fretting fatigue of 35CrMoA steel, but levels of variables were quite limited in that study, which didn't perform an integrated research on the fretting fatigue behavior of 35CrMoA steel. Moreover, the comparison of the strain response behavior under different paths was limited, the explanation of the fretting zone wear mechanism was incomplete, and the analysis of crack initiation and propagation was lacking.

In this paper, 35CrMoA steels were both used as the specimens and the fretting pads, and the contact form of the cylindrical surface was used to explore the multiaxial fretting fatigue behavior and mechanism of 35CrMoA steel under the square path (SP) and diamond path (DP). The research analyzed the strain response under different loading paths during fretting fatigue, compared the morphology of the fretting area under different contact stresses and different loading paths. The abrasive debris in slip region and stick region of the SP was examined to analyze the composition and describe the process of abrasive debris generation. Moreover, the fretting fatigue fracture morphology was observed to analyze fracture features of crack source zone (CSZ), crack propagation zone (CPZ) and instantaneous fracture zone (IFZ). The cracks' initiation and propagation were also concluded from the fracture morphology.

EXPERIMENTAL PROCEDURES

The samples and fretting pads materials used in this experiment were 35CrMoA steel. The heat treatment processes used for fretting fatigue specimens and fretting pads were quenching and tempering. The specific treatment processes were: solution treated at 850 for 25min in a box type resistance furnace, quenched in oil, and followed immediately by aging at 550 for 1 hour, finally cooling in oil. The chemical composition and main mechanical properties of the 35CrMoA steel are shown in Tab.1 and Tab.2, respectively.

Table1 Chemical composition of 35CrMoA steel (wt %)

C	Cr	Mo	Mn	Si	P	S	Fe
0.32-0.39	0.8-1.10	0.15-0.25	0.4-0.7	0.17-0.37	0.013	0.006	Balance

Table2 The main mechanical properties of 35CrMoA steel

Yield Strength /MPa	Tensile Strength /MPa	Young Modulus /GPa	Elongation /%	Reduction in Area/%	Hardnes
1040	1375	205	12	17	17

Fig. 1 shows the dimensions of the sample and the fretting pad. After processing of the sample and the fretting pad, 1 #, 2 #, 3 #, 4 # SiC sandpapers were used in sequence to polish the gauge section of the sample and the fretting pad contact surface, in which polishing direction is along the axial direction of the sample. The polished surface roughness (Ra) was no more than 0.16.

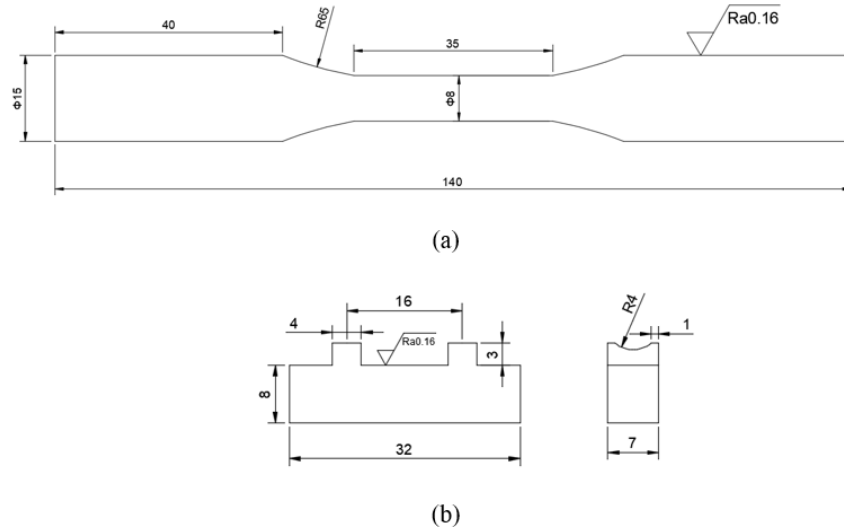


Fig.1 The dimensions of the sample and the fretting pad (a) sample;(b) fretting pad (unit: mm)

The fretting fatigue experiment was performed using a MTS809 tension-torsion combined electro-hydraulic servo fatigue testing system. The equivalent cyclic stress (σ_e) was 400MPa. The contact stress (P) was 50MPa, 150MPa, 250MPa respectively. The loading paths were DP and SP. Two fretting pads were symmetrically fixed to both sides of the sample by screws, and a ring-type load cell was used to clamp the fretting pad to the sample for changing and measuring the contact stress. The diagrams of fretting pad clamping device are shown in Fig. 2. Both axial and torsional directions were cyclically loaded in square waves with a stress amplitude ratio of -1. The axial and torsional frequencies were 3Hz with a phase difference of 90°. The strain change of the sample during the test was measured by the strain sensor. When the measured strain exceeded a certain set value, the experiment was automatically stopped.

In this paper, the micro-morphology, fracture morphology and wear debris composition of the fretting area were analyzed. The morphology observations were conducted by using the FEI Quanta200F scanning electron microscope (SEM) and the composition of the wear debris were detected by using the energy dispersive X-ray spectrometer (EDX).

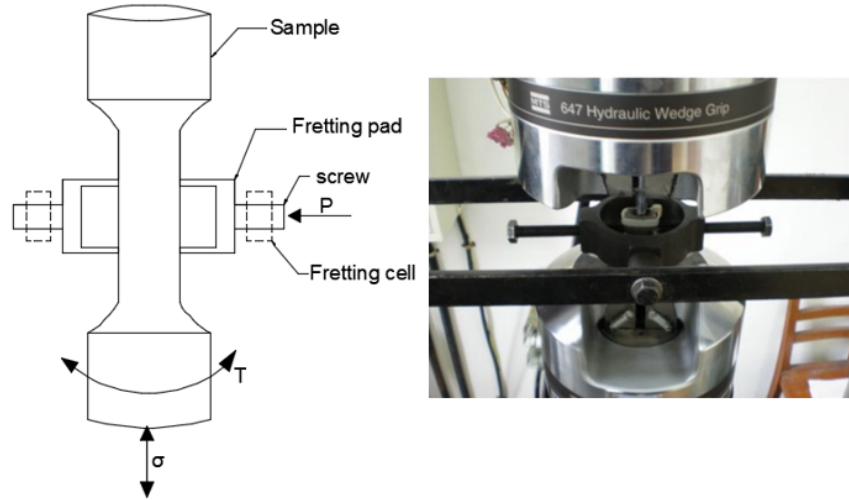


Fig.2 Diagrams of fretting pad clamping device

1. RESULTS AND DISCUSSION

2. Strain response behavior

During the fretting fatigue process, due to the effect of alternating stress, the phenomenon of "cyclic hardening" or "cyclic softening" frequently occurred. The phenomenon of cyclic hardening or cyclic softening depended on the original state of the material, crystal structure, strain amplitude (stress amplitude), and the working environment of the material; At the micro level, it was related to the dislocation structure, dislocation density, and stacking fault energy in the material.²⁷⁻²⁹ G.Z.kANG et al.³⁰ found that 40Cr3MoV bainitic steel showed cyclic softening in uniaxial cyclic loading after certain cycles and no stable state existed if strain amplitude was higher than 0.9%. 35CrMoA steel also experienced cyclic softening during multiaxial composite fretting fatigue. Fig. 3 shows the equivalent strain response behavior of 35CrMoA steel under SP and DP with the equivalent stress of 400MPa. It can be clearly seen that in the first 300 cycles of the square path, the equivalent strain (ϵ_e) gradually increases with the same equivalent stress, different degrees of cyclic softening occur. When it reaches 300 cycles, the equivalent strain basically stabilizes in each condition, and the cyclic softening phenomenon disappears meanwhile. After the fretting fatigue cycle reaches 7000 cycles, the equivalent strain is slightly reduced, and the material is strengthened internally, and a lesser degree of cyclic hardening occurs; Under the DP, the material shows a continuous cyclic softening trend. As the number of fretting fatigue cycles increases, its cyclic softening rate gradually decreases, and cyclic hardening does not occur in the later stage of fretting fatigue, and as the contact stress increases the slower the cyclic softening rate decreases.

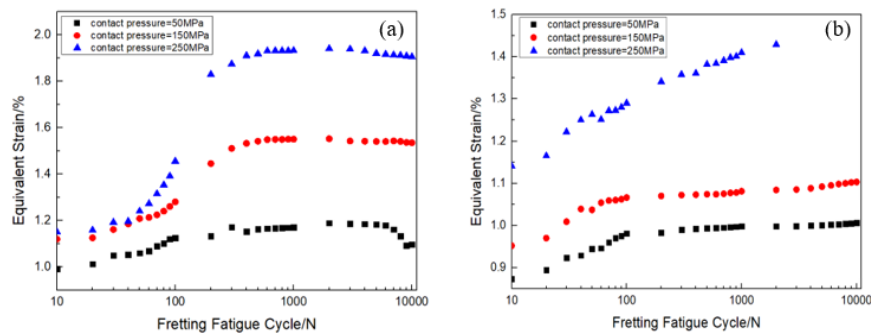


Fig.3 Curves of the change of equivalent strain with cycles (a) SP;(b) DP

Under SP and DP, the changed trend of equivalent strain before and after 300 cycles is quite different (Fig.3). Fig. 4 is a histogram of the equivalent strain of 35CrMoA steel with different contact stresses under SP and DP at the 10th, 100th, 200th, and 300th cycles.

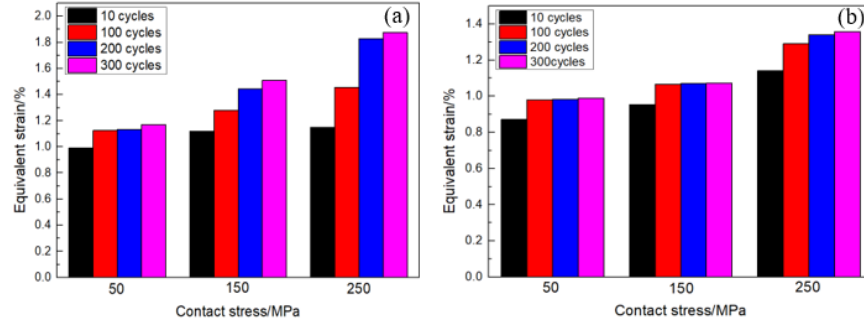


Fig.4 Equivalent strain histograms for the 10th, 100th, 200th, and 300th cycles (a) SP;(b) DP

As shown in Fig. 4, the height difference between any two columns under the same contact stress displays the equivalent strain change value between the corresponding cycles. The change rate of equivalent strain is obtained from this height difference. Under SP and DP, the cyclic softening rate decreases with the increase of the cycle number, and the strain change rate increases as the contact stress increases. Combined Fig. 3 and Fig. 4, the SP has a larger amount of strain under the same conditions and its cyclic softening rate is also larger compared with DP.

Fig. 5 shows the response behavior of axial strain and shear strain of 35CrMoA steel under SP and DP at the equivalent stress of 400MPa. The axial strain and the shear strain are basically the same as the equivalent strain change trend. This change trend has been described in the analysis of equivalent strains. Corresponding to the equivalent strain, under the same conditions, the shear strain, axial strain and their change rates of SP are larger than DP. Compared with the shear strain, the axial strain dominates the total strain. During the cyclic softening process, the increase of the axial strain is much larger than the increase of the shear strain. Therefore, the damage form of 35CrMoA steel is mainly axial style.

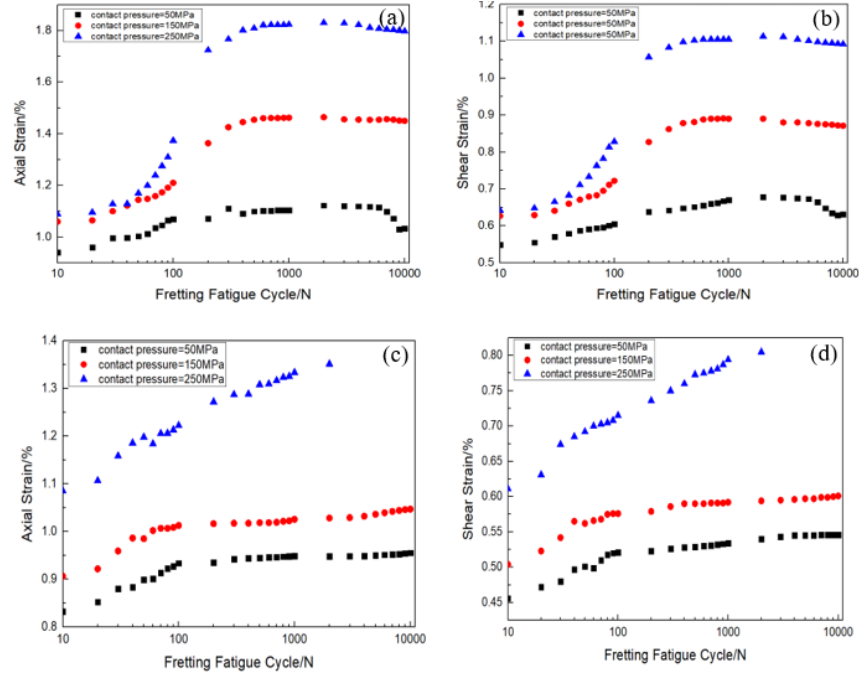


Fig.5 Changes in axial strain and shear strain with cycles (a) (b) SP;(c) (d) DP

Fretting fatigue life

In this experiment, fretting fatigue studies of 35CrMoA steel with contact stresses of 50 MPa, 150 MPa, and 250 MPa were performed under SP and DP. The obtained fretting fatigue life is shown in Tab.3;

Table3 Fretting fatigue life of SP and DP under different contact stresses

Path	Contact stress/MPa	Fretting fatigue life/Cycles
SP	50	17268
	150	14624
	250	10270
DP	50	15382
	150	14288
	250	2620

The fretting fatigue life gradually decreases with increasing contact stress under SP and DP. The study by Liu et al.²⁴ showed multiaxial fretting fatigue life of 35CrMoA steel had a trend of decreasing first, then increasing and finally decreasing with increasing contact stress. With the same contact stress range, the same trend of fretting fatigue life was achieved in this paper. Compared with plain fatigue, the contact stress was added between the fretting pad and the specimen during the fretting fatigue, which caused the fretting wear on the surface of the specimen. The larger the contact stress, the more severe the surface damage of the specimen, and the stress concentration was more obvious in this situation, which accelerated the initiation and propagation of microcracks and reduced the fretting fatigue life.^{23,31} As the contact stress of 35CrMoA steel increased, the equivalent strain also increased, indicating that the sample had undergone severe plastic deformation during the fretting fatigue process. At this situation, serious fretting wear occurred, so the greater the contact stress, the more serious the surface damage of the sample, the more obvious the stress concentration phenomenon, which led to a faster crack initiation rate, and greater plasticity also accelerated

crack propagation; In addition, at the beginning of fretting fatigue, there was adhesive wear between the specimen and the fretting pad. When the adhesive part was torn due to fretting, fine metal debris was generated.³² This process gone on and the debris continued to increase, which caused the change of fretting wear from adhesive wear to abrasive wear. After the fretting surface was wiped by the abrasive wear, the surface microcracks may be erased, thereby reducing the source of cracks and improving the fretting fatigue life.^{33,34} The greater the contact stress, the lower the relative displacement between the specimen and the fretting pad, which reduced the wiping effect of abrasive wear on microcracks, resulting in a low fretting fatigue life. Combining the above two reasons, the fretting fatigue life of 35CrMoA steel under SP and DP showed a downward trend with increasing contact stress. Under the same contact stress and equivalent stress, the fretting fatigue life of DP was slightly lower than the fretting fatigue life of SP. The fretting fatigue damage of the 35CrMoA steel was greater under DP.

Analysis of fretting region

3.3.1 Morphology of fretting region

During the fretting fatigue process of the material, the fretting wear occurred on the contact surface between the specimen and the fretting pad due to contact stress and cyclic stress. Under different contact stresses, the fretting region showed different morphology. Fig.6 presents the morphology of the fretting region of 35CrMoA steel with different contact stresses under DP and SP;

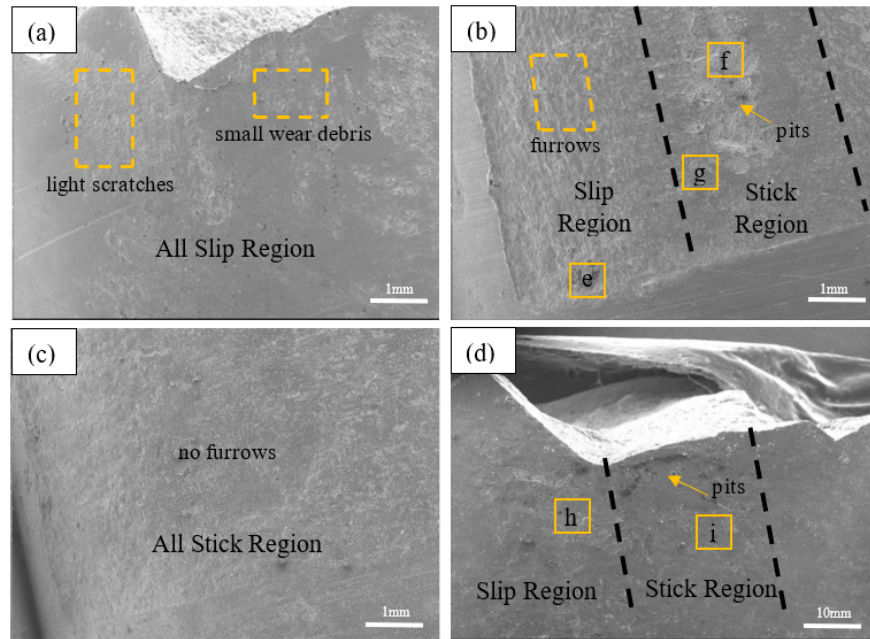


Fig.6 Morphology of fretting region; (a) P=50 MPa, (b) P=150 MPa, (c) P=250 MPa, DP, $\sigma_e = 400\text{MPa}$; (d) P=150MPa, SP, $\sigma_e = 400\text{MPa}$.

Under DP, when the contact stress is 50 MPa, which is a relatively low value, the amount of deformation caused by the fretting of the sample and the fretting pad is limited, the relative displacement is large, and the fretting process is nearly in the slip regime, as shown in Fig.6 (a), although there are a large number of scratch marks and micro abrasive debris, the scratch marks are shallow, and the deformation and damage in the fretting region are not very severe; With the increase of contact stress, the adhesion between the specimen and the fretting pad is too close to reduce the relative displacement. Compared with low contact stress, the fretting region has deeper scratch marks, and the surface of the fretting region is severely worn. When the contact stress is 150 MPa, as shown in Fig.6 (b), a partial stick area has appeared in the center

of the fretting region and there is an obvious furrow phenomenon in the slip area; When the contact stress is further increased to 250 MPa, the fretting region is then basically in an stick state, as shown in Fig.6 (c), there are no furrows due to sliding. Due to lower contact stress, the relative displacement in Fig.6 (b) is larger compared to Fig.6 (c). During the fretting fatigue process, part of the material in the adhesion area tears due to the large relative displacement. As a result, the surface material of the fretting region is torn in Fig.6(b), and a large number of pits are generated. By compared with Fig.6 (c), Fig.6 (b) is more severely damaged due to the severe tearing of the surface material and the coupling effect with the fretting wear.

Under SP, as the contact stress increases, the surface wear of the fretting zone also becomes more serious. Compared with the morphology of the fretting zone of the DP, due to the larger amount of strain under the same conditions under SP, there is a relatively large amount of relative displacement. Therefore, under the same contact stress, the adhesion of SP is lower, and surface tearing is weaker than that of the DP. When the contact stress is 150 MPa, stick and slip regions can also be observed on the surface of the fretting zone. There are more abrasive debris in the slip region and a small amount of surface material tear in the stick region.

3.3.2 Analysis of stick and slip regions

The morphology of the stick region and the slip region with an equivalent stress of 400 MPa and a contact stress of 150 MPa under DP is shown in Fig.7(e)(f)(g);

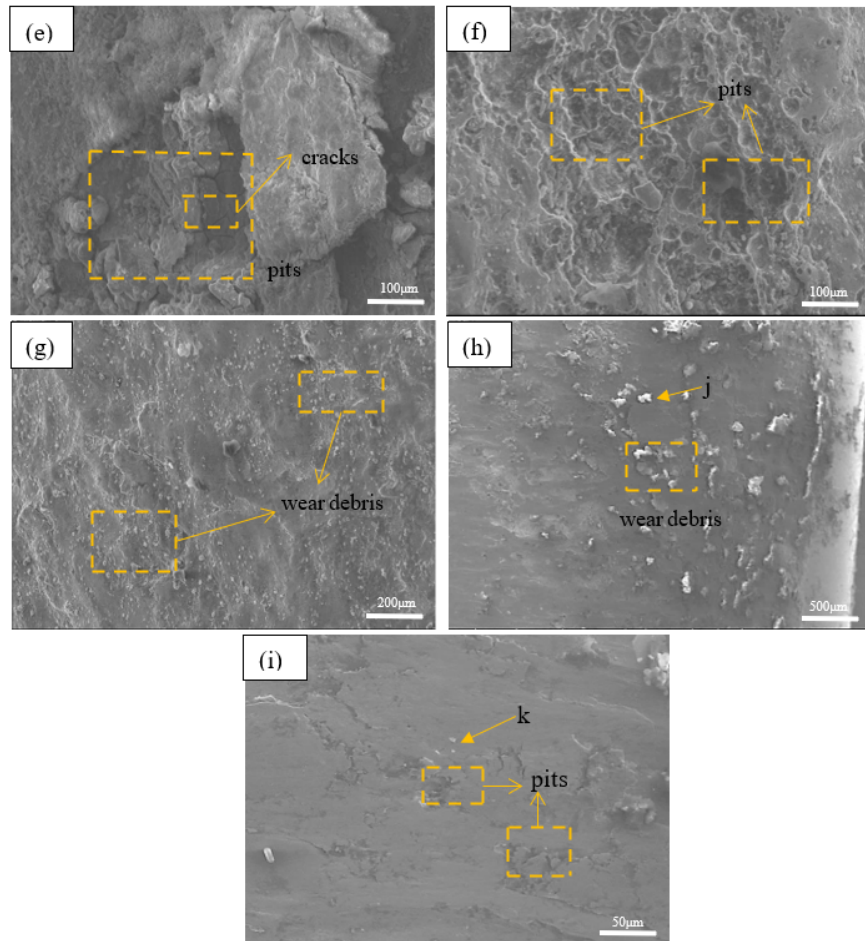


Fig.7 amplified images of the slip and stick regions in Fig.6(b) and Fig.6(d)

The surface of the sample continuously undergoes plastic deformation due to the fretting friction between the sample and the fretting pad in the slip region. After repeated sliding, rolling, and smoothing, plastic failure occurs on the surface. Lamellar spalling occurs in the slip zone, forming pits and wear debris with different depths and shapes. The overall damage in the slip region is relatively large, the scratches are deep, and the surface is extremely rough. Because of the wiping effect of abrasive particles on the surface of the slip region, there are almost no microcracks on the normal surface, and the microcracks occur only at the edges of the pits where stress is concentrated. Kozo Nakazawa et al.²³ made similar findings in their research. In the stick region, due to the coupling effect of adhesion and fretting, the surface material of the sample is severely torn, and many small pits are connected to form a large pit. The surface damage is small in the stick region where no tearing of the surface material has occurred, and basically no slip marks similar to the slip region.

The morphology of the stick region and the slip region with an equivalent stress of 400 MPa and a contact stress of 150 MPa under SP is shown in Fig7.(h)(i); There are a lot of abrasive debris in the slip region of SP, and furrows caused by the sliding effect can be seen everywhere, and the surface is very rough; The surface of the stick region is smoother than that of the slip region, and the surface is free of scratches caused by the sliding effect, but there are pits of different shapes caused by the surface material tearing. Compared with DP, the area and depth of the pits generated in SP are less.

3.3.3 Composition analysis of wear debris in fretting region

The conditions and mechanisms for the generation of wear debris in the fretting region under SP and DP are basically the same. In this study, the components of the wear debris in the slip zone and the stick region were investigated taking SP as an example. Fig.8(j)(k) are the EDX spectrums of the wear debris component in the slip region and the stick region when the contact stress is 150 MPa and the equivalent stress is 400 MPa under SP;

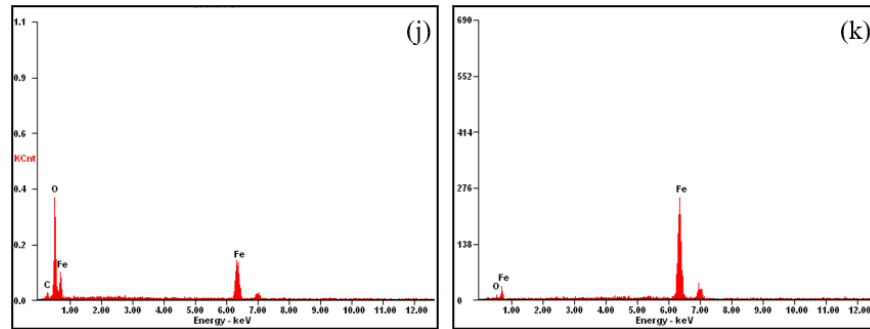


Fig.8 EDX spectrums of wear debris in slip and stick region under SP, (j) slip region;(k) stick region.

The EDX spectrum shows that there is a huge difference in the oxygen content of the wear debris between the slip region and the stick region. Obviously, the oxygen content in the slip region is higher than that of in the stick region. The oxygen of wear debris in slip region is thought to come from the oxidation of the steel which is caused by a huge amount of heat out of the fretting and friction between the sample and the pad in the contact stress condition. The wear debris is considered to be a mixture of sample material and its oxide in the slip region. The oxygen content of the stick region is very low, which indicates that there is little oxidation of the sample in the stick region. The wear debris is basically composed of the sample material in the stick region. Since the slip region is located at the edge of the fretting zone and the relative displacement occurs between the sample and the fretting pad, the oxidation becomes very easy with sufficient oxygen; The stick region is located in the middle of the fretting zone, and its relative displacement is quite small, which would cause an insufficient oxygen environment, so the degree of oxidation is extremely low. A number of researchers had focused on the oxidation of wear debris during fretting fatigue. Wang et al.¹ had reported

the chemical composition of fretting debris of AlSi9Cu2Mg Alloy. Peng et al.¹⁵ had analyzed the oxidation degree of the sample's loading side, center position and fixed side respectively, and found that the oxidation was uneven.

1. **Fretting fatigue fracture analysis**
2. **Macro Fracture Analysis**

Due to the effects of diverse factors, the fracture morphology shows unique features. The combination of contact stress and cyclic stress may change the crack initiation position and propagation path. The macro fracture morphology of the equivalent stress of 400 MPa under SP and DP are shown in the Fig.9;

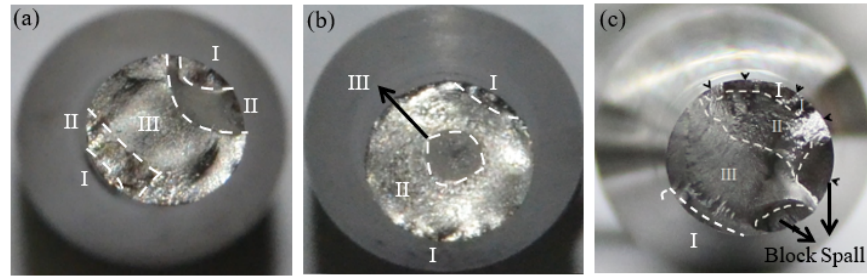


Fig.9 Macro fracture morphology; (a) P=50MPa, DP; (b) P=250MPa, DP; (c) P=150MPa, SP; $\sigma_e=400\text{MPa}$.

The fretting fatigue fracture of 35CrMoA steel basically includes three characteristic regions, named with the crack source zone (CSZ), crack propagation zone (CPZ) and instantaneous fracture zone (IFZ) (respectively I, II, III). When the contact stress is low, the proportion of CSZ and IFZ is large, and although CSZ is generated in the two corresponding fretting regions, there is always a CSZ that predominates during the crack propagation, which would make IFZ biased towards another CSZ; With the increase of contact stress, the fracture area occupied by CSZ and IFZ is reduced. In the whole fracture area, CPZ occupies the main parts, and the cracks generated by the two corresponding fretting regions both dominate, so that IFZ is located in the center of the fracture and always has a nearly symmetrical shape. When the contact stress is large, the amount of deformation generated by the sample and the stress concentration at the material damage caused by fretting are larger, so microcracks are easier to form and are more liable to propagate into main cracks under this action. Therefore, CSZ of fracture under high contact stress is small and shows good symmetry.

Compared with DP under the same conditions, there are multiple crack source regions in the fretting fatigue fracture under SP, but there is also only one main crack source region, and block spall of the material also occur in the fracture area. This is due to the fact that the main crack spreads to connecting with the microcracks that are not generated at the same level, which causes the material to fall off.

Micro fracture analysis

Fig.10 is the fretting fatigue fracture morphology under DP with equivalent stress of 400MPa and contact stress of 50MPa. The CSZ, CPZ and IFZ can be clearly distinguished from the figure. Within a certain number of cyclic cycles after crack initiation, it mainly expands in the cross section of the specimen. At this situation, although the specimen is also subjected to the combined effect of contact stress and equivalent cyclic stress, the microcrack is closer to the surface of the fretting zone. Therefore, it is mainly controlled by contact stress; When the crack grows to a certain length, which is far from the surface, the effect of cyclic stress on the crack growth gradually strengthens, so that the crack propagation appears along the longitudinal component, and as the crack further expands, the longitudinal rate of crack propagation increases gradually. Fretting fatigue fracture surface continuously produces stairs along the longitudinal direction.

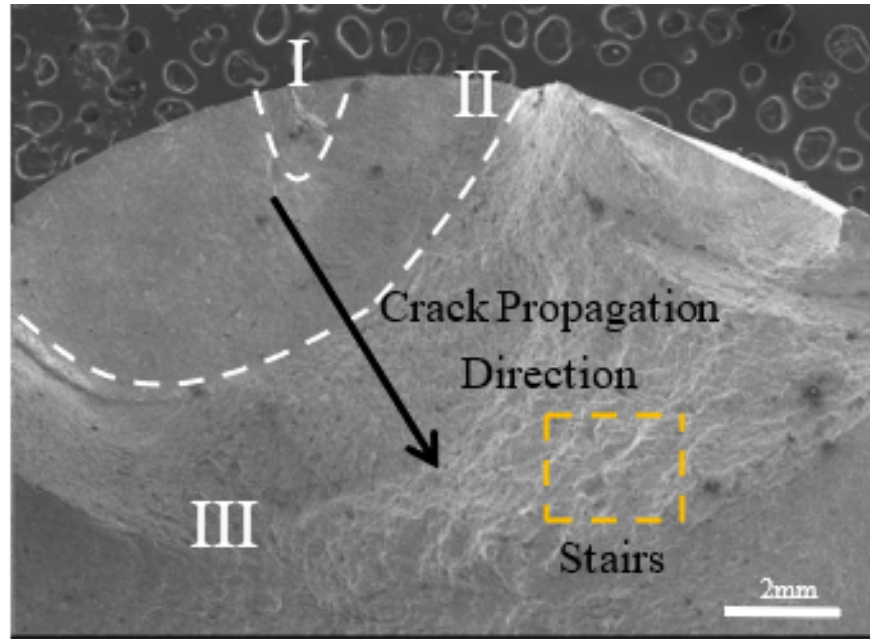


Fig.10 Micro fracture morphology under DP, $P=50\text{MPa}$, $\sigma_e=400\text{MPa}$.

The amplified morphologies of areas I, II, and III in Fig.10 are shown in Fig.11;

There are obvious cracks in the CSZ, and due to the combined effect of axial stress and torsional stress, the cracks are tortuous, as shown in Fig.11(a). In addition to the main crack, there are multiple secondary cracks around the main crack. The CPZ is between the CSZ and IFZ, and fatigue striation is the main feature due to the repeated open and closure of the cracks, therefore many grooves are formed here, as shown in Fig.11(b). The IFZ is formed due to the instability propagation of the crack. Since the formation of this characteristic region is instantaneous, stairs are often formed along the crack propagation direction on the fracture surface, as shown in Fig.11(c).

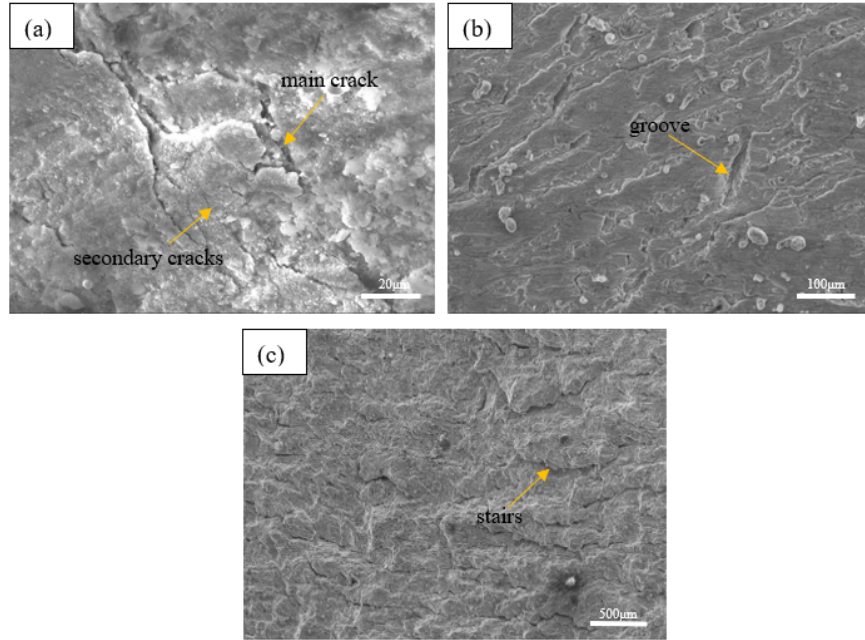


Fig.11 Amplified morphologies of the CSZ, CPZ and IFZ under DP, $P=50\text{MPa}$, $\sigma_e=400\text{MPa}$; (a) CSZ; (b) CPZ; (c) IFZ.

Fig.12 shows the amplified morphologies of the CSZ, CPZ and IFZ under SP; It can be found that the crack source is located at the subsurface of fretting region from the CSZ, as shown in Fig.12(a). Similarly, the crack is tortuous, and multiple secondary cracks are around the main crack. In the CPZ, the steady propagation of cracks has appeared, and a number of small secondary cracks have also extended on the main crack, as shown in Fig.12(b). These secondary cracks have a small size due to the large propagation resistance. The IFZ is shown in Fig.12(c), the morphological features are significantly different from the IFZ under DP. Under SP, a radial cross section appeared in the IFZ. Radial cross-section is formed by the intersection of crack fronts when the cracks rapidly expand at different heights, and there are also obvious dimple patterns in the IFZ, as shown in Fig.13.

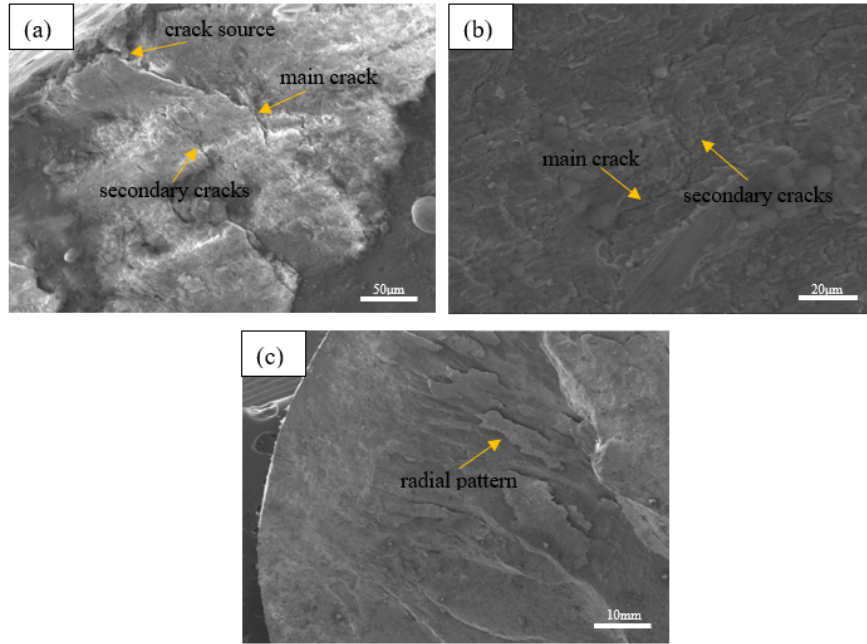


Fig.12 Amplified morphologies of the CSZ, CPZ, and IFZ under SP, $P=50\text{MPa}$, $\sigma_e=400\text{MPa}$; (a) CSZ; (b) CPZ; (c) IFZ.

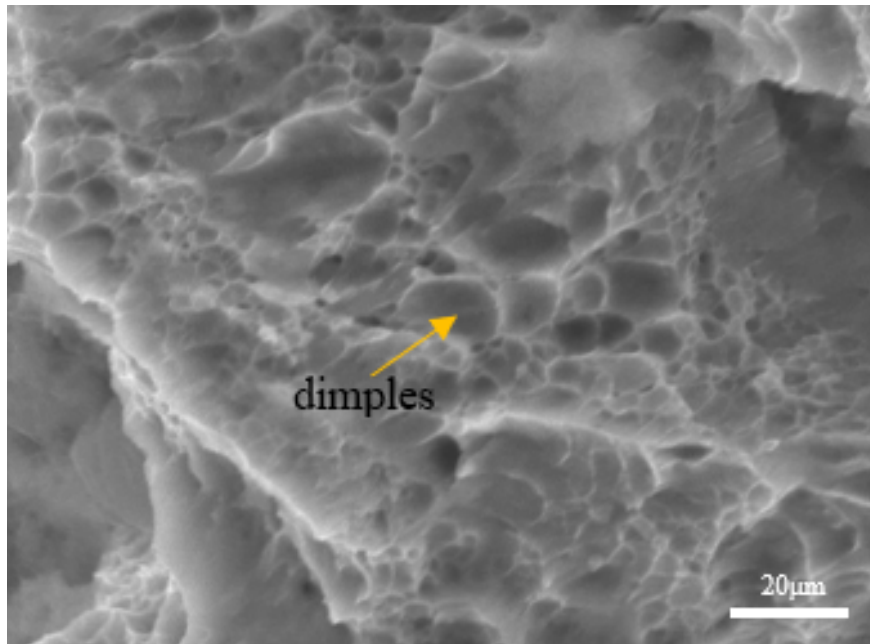


Fig.13 Dimple patterns in the IFZ.

CONCLUSIONS

Based on the morphology observation and multiaxial fretting fatigue test on 35CrMoA steel, the following conclusions can be drawn:

1. Under different loading paths, the strain response behavior of 35CrMoA steel is significantly different. However, contact stress has the same effect on the cyclic softening rate under different loading paths. The greater the contact stress, the greater the cyclic softening rate. Moreover, the axial strain and the rate of change in axial strain dominates in the whole strain. Therefore, the main damage form under the two paths is axial style.
2. Under SP and DP, the fretting fatigue life of 35CrMoA steel shows a downward trend with increasing contact stress. In this process, large plastic deformation and abrasive wear wiping microcracks play a dominant role.
3. With a contact stress of 150 MPa under DP, the damage in the fretting area is the most serious, a large amount of material tear appeared in the stick zone, and the crack in the slip area only initiates at the edge of the pit; Wear debris basically consists of sample material and its oxide, but the oxidation portions of the sample material in the slip zone are much higher than those in the stick zone.
4. With the increase of contact stress, the area of CSZ and IFZ in the fretting fatigue fracture gradually decreased; At low contact stress, only one CSZ dominates in the two corresponding fretting regions; At high contact stress, cracks generated in both fretting regions are dominant, and the IFZ is symmetrical nearly circular shape.
5. Within a certain number of cycles (including the crack initiation and propagation stage), the crack first propagates in its initiating cross section, where the crack propagation is mainly affected by contact stress; As the crack grows, when reached to a certain depth, a longitudinal component will be generated during the crack growth. At this situation, the cyclic stress has a significant effect on crack growth. As the crack depth becomes deeper, the longitudinal component becomes larger.

ACKNOWLEDGEMENTS

The authors would like to express sincere thanks for the financial support by the National Basic Research Program (973Program) through Research Grant NO. 2007CB714704 and the National Natural Science Foundation of China through Research NO. 50771073.

References

1. Wang J, Xu H, Su TX, Zhang Y, Guo Z, Mao HP et al. Fretting Fatigue Experiment and Analysis of AlSi9Cu2Mg Alloy. *Materials*. 2016;9: 984.
2. Majzoobi GH, Jaleh M. Duplex surface treatments on AL7075-T6 alloy against fretting fatigue behavior by application of titanium coating plus nitriding. *Mater Sci Eng A*. 2007;452-453: 673-681.
3. Hills DA, Nowell D, O'Connor JJ. On the mechanics of fretting fatigue. *Wear*. 1988;125(1-2): 129-146.
4. Pape JA, Neu RW. A comparative study of the fretting fatigue behavior of 4340 steel and PH 13-8 Mo stainless steel. *Int J Fatigue*. 2007;29(12): 2219-2229.
5. Madge JJ, Leen SB, Shipway PH. A combined wear and crack nucleation-propagation methodology for fretting fatigue prediction. *Int J Fatigue*. 2008;30(9): 1509-1528.
6. Giummarra C, Bray GH, Duquette DJ. Fretting fatigue in 2XXX series aerospace aluminium alloys. *Tribol Int*. 2006;39(10): 1206-1212.
7. Hattori T, Yamashita K, Yamashita Y. Simple estimation method of fretting fatigue limit considering wear process. *Tribol Int*. 2017;108: 69-74.
8. Wang WJ, Wang M, Yang GX, Xie JL. Experimental Investigation of Fretting Fatigue of Train Axles under Rotating Bending. *Adv Mater Res*. 2011;291-294: 1110-1115.
9. Benhamena A, Amrouche A, Talha A, Benseddig N. Effect of contact forces on fretting fatigue behavior of bolted plates: Numerical and experimental analysis. *Tribol Int*. 2012;48: 237-245.
10. Gnanamoorthy R, Reddy RR. Fretting fatigue in AISI 1050 steel. *Bull Mater Sci*. 2002;25(2): 109-114.
11. Berthier Y, Colombé Ch, Vincent L, Godet M. Fretting Wear Mechanisms and Their Effects on Fretting Fatigue. *Int J Tribol*. 1988;110(3): 517-524.
12. Xiang XY, He GQ, Liu B, Hu ZF, Zhu MH. Overview of Factors Influencing Fretting Fatigue of Wheel Axle of High-speed Train. *Mater Rev*. 2009;23(1): 63-66.
13. Shinde SR, Hoepfner DW. Fretting fatigue behavior in 7075-T6 aluminum alloy. *Wear*. 2006;261(3-4):

- 426-434.
14. Yang MS, Zhao HQ, Wang YX, Chen XF, Fan JL. Study on fatigue life of aluminum alloy considering fretting. *Mater Sci Eng*. 2018;(301): 012087.
 15. Peng JF, Wang BT, Jin X, Xu ZB, Liu JH, Cai ZB et al. Effect of contact pressure on torsional fretting fatigue damage evolution of a 7075aluminum alloy. *Tribol Int*. 2019;137: 1-10.
 16. Navarro C, García M, Domínguez J. A procedure for estimating the total life in fretting fatigue. *Fatigue Fract Eng Mater Struct*. 2003;26(5): 459-468.
 17. Talemi RH, Wahab MA. Finite Element Analysis of Localized Plasticity in Al 2024-T3 Subjected to Fretting Fatigue. *Tribol T*. 2012;55(6): 805-814.
 18. Zhou ZR, Nakazawa K, Zhu MH, Maruyama N, Kapsa Ph, Vincent L. progress in fretting maps. *Tribol Int*. 2006;39(10): 1068-1073.
 19. Shinde S, Hoepfner DW. Quantitative analysis of fretting wear crack nucleation in 7075-T6 aluminum alloy using fretting maps. *Wear*. 2005;259(1-6): 271-276.
 20. Feng XY, Dong SY, Yan SX, Liu XT, Xu BS, Pan FS. Heat-affected zone microstructure and mechanical properties evolution for laser remanufacturing 35CrMoA axle steel. *Proc. of SPIE*. 2017;10710: 107103P-1.
 21. Farrahi GH, Minaia K, Bahai H. Fretting fatigue behavior of 316L stainless steel under combined loading conditions. *Int J Fatigue*. 2019;128: 105206.
 22. Teng ZJ, Liu HQ, Wang QY, Huang ZY, Starke P. Fretting behaviors of a steel up to very high cycle fatigue. *Wear*. 2019;438-439: 203078.
 23. Nakazawa K, Maruyama N, Hanawa T. Effect of contact pressure on fretting fatigue of austenitic stainless steel. *Tribol Int*. 2003;36(2): 79-85.
 24. Liu B, He G, Jiang X, Zhu M. Multi-axial fretting fatigue behavior of 35CrMoA steel. *Fatigue Fract Eng Mater Struct*. 2011;34(12): 974-981.
 25. Tian DD, He GQ, Shen Y. The fretting fatigue behavior of 35CrMoA under square and diamond paths. *J Func Mater*. 2016;47(5): 5078-5083.
 26. Lv SQ, He GQ, Shen Y. Fretting Fatigue Behavior of 35CrMoA Steel Under Diamond Loading Condition. *J Mater Eng*. 2016;44(1): 96-102.
 27. Zhang ZP, Li J, Sun Q, Qiao YJ, Li CW. Two Parameters Describing Cyclic Hardening/Softening Behaviors of Metallic Materials. *J Mater Eng Perform*. 2009;18: 237-244.
 28. Laird C, Buchinger L. Hardening behavior in fatigue. *Metall Trans A*. 1985;16: 2201-2214.
 29. Shang HX, Ding HJ. Low cycle fatigue stress-strain relation model of cyclic hardening or cyclic softening materials. *Eng Fract Mech*. 1996;54(1): 1-9.
 30. Kang GZ, Li Y, Gao Q, Kan QH, Zhang J. Uniaxial ratchetting in steels with different cyclic softening/hardening behaviours. *Fatigue Fract Eng Mater Struct*. 2006;29(2): 93-103.
 31. Jayaprakash M, Mutoh Y, Asai K, Ichikawa K, Sukarai S. Effect of contact pad rigidity on fretting fatigue behavior of NiCrMoV turbine steel. *Int J Fatigue*. 2010;32(11): 1788-1794.
 32. Zhang DK, Ge SR, Qiang YH. Research on the fatigue and fracture behavior due to the fretting wear of steel wire in hoisting rope. *Wear*. 2003;255(7-12): 1233-1237.
 33. Shen Y, Zhang DK, Duan JJ, Wang DG. Fretting wear behaviors of steel wires under friction-increasing grease conditions. *Tribol Int*. 2011;44(11): 1511-1517.
 34. Wang DG, Zhang DK, Ge SR. Fretting-fatigue behavior of steel wires in low cycle fatigue. *Mater Des*. 2011;32(10): 4986-4993.